J Solid State Electrochem (2017) 21:2791–2798
DOI 10.1007/s10008-017-3605-4

ORIGINAL PAPER

Enhanced catalytic activity of ppy-coated pencil electrode in the presence of chitosan and Au nanoparticles for hydrogen evolution reaction

Didem Balun Kayan[1] · **Derya Koçak**[1]

Received: 18 November 2016 / Revised: 11 April 2017 / Accepted: 12 April 2017 / Published online: 26 April 2017

Abstract Catalytically active and low-cost electrocatalysts for the production of hydrogen from water are extremely important for future renewable energy systems. Here, we report the fabrication of a facile pencil graphite electrode modified with polypyrrole-chitosan/Au nanoparticles and tested its performance for electrocatalytic hydrogen evolution reaction (HER) as a model process. The porous surface of the pencil graphite electrode (PGE) was modified potentiostically by polypyrrole (PPy) at various film thicknesses in the presence of chitosan (Chi), which is a natural biopolymer, in the electrolyte medium. After the optimum film thickness had been obtained, the Au particles electrodeposited on to the PPy/Chi composite film at the nano-scale to benefit both from its well-known high catalytic activity and to reduce the amount of precious metal Au to prepare a low-cost eletrocatalyst. The performance of this composite catalyst on the H^+ reduction (H_{ad} formation) and thereby on the hydrogen evolution was investigated. Data from cyclic voltammetry (CV), Tafel polarization curves, and electrochemical impedance spectroscopy (EIS) demonstrated that the current densities related to the electron transfer rate changed with the thickness of the composite film, and the catalytic activity was enhanced more with deposition small amount of Au on to the catalyst surface.

Keywords Conducting composite · Pencil graphite · Chitosan · Au nanoparticles · Hydrogen evolution reaction

✉ Didem Balun Kayan
didembalun@aksaray.edu.tr

[1] Department of Chemistry, Science and Arts Faculty, Aksaray University, 68100 Aksaray, Turkey

Introduction

Increasing energy requirements due to industrial and population growth has made the traditional energy resources, like fossil fuels, insufficient. Hydrogen seems to be an ideal candidate as a carbon-free fuel due to its high energy density. The production of molecular hydrogen by the electrochemical reduction of water is an important part of several clean energy technologies [1–14]. A practical and sustainable way to produce hydrogen is by the electrolysis of water, but this has one disadvantage due to an overpotential occurring in the electrochemical system, which increases the cost of the method. Although some noble metals, such as Pt, Au and Rh, are known as good hydrogen evolving catalysts in acidic solutions, the high cost of these metals limits their large-scale application. Therefore, cost-effective materials for the electrochemical production of hydrogen are a central area of the research into renewable energy. In addition to being low-cost, it is a challenge to develop highly active catalysts that are stable for long periods. From this point of the view, due to it being electrochemically active, low-cost, commercially available, mechanically rigid, easy to modify and especially having a large active surface area due to its porous structure, the pencil graphite electrode is an appropriate material for hydrogen production as in many other electrocatalytic applications [15–19].

Conducting polymers are materials that have intrinsic properties that are of interest to many fields of research related to electrochemistry. Among all the conducting polymers, polypyrrole has become the most commonly used due to its considerable electrical conductivity, stability, ease of synthesis and treatment. The surface of thin films of the conducting polymers/composites can be a supporting material for metal nanoparticles and provides a much larger effective surface area than bare metal electrodes due to their rough surfaces.

In addition, the metal particles that dispersed homogeneously on this surface offer an increase in the intrinsic electrocatalytic activity of the hydrogen evolution [19–22].

Many attempts have been made to apply the highly conductive, catalytic, sensor and mechanical properties of the conducting polymers to different practical needs through blending or composite formation. For this purpose, chitosan, which is the second most abundant and renewable biopolymer after cellulose, has been used in a wide range of research areas. It possesses a unique combination of structural, mechanical, catalytic and thermal properties, as observed in numerous composites [23–28].

Nano-scale materials have excellent catalytic activities because of their active surface areas, which results in unique physical, chemical and biological properties that differ essentially from the properties of larger particles [26, 29].

In this study, we present a method for the fabrication of a catalyst by modifying a low-cost, low-technology and mechanically rigid pencil graphite electrode and used it in hydrogen evolution as a model process to demonstrate its catalytic activity. The other and the most important reason choosing the pencil graphite was its easy commercial availability. The modification was performed by codeposition of polypyrrole using the abundant natural biopolymer chitosan as the raw material. Then, we used this polymeric surface for the electrodepositon of gold metal particles at the nano-scale, which exhibit high catalytic activity in hydrogen evolution [30, 31]. Using this efficient catalyst at the nano-scale considerably reduced the amount of Au in the catalyst, resulting in low cost of prepared catalyst. To the best of our knowledge, pencil graphite as the carbon-based electrode modified by PPy-Chi/Au, prepared and used for hydrogen production fromwater for the first time in the literature. The performance of PPy-Chi/Au composite film was examined by electrochemical techniques. Designing a stable catalyst for long-term use was another goal of this study. The catalytic activity of the PGE modified by the PPy-Chi/Au was maintained over 6 h of electrolysis with a current density of nearly 80 mA cm^{-2}.

Experimental

The pyrrole monomer (Merck) was purified by distillation under reduced pressure prior to use. Chitosan (medium molecular weight) was purchased from Sigma-Aldrich, oxalic acid, hydrochloric acid, sulphuric acid and chloroauric acid ($HAuCl_4$) were purchased from Merck, and all were used as received without any further purification. Aqueous solutions were prepared daily with ultrapure water. The electropolymerization solutions were prepared in a 0.3 mol L^{-1} oxalic acid solution containing 0.1 mol L^{-1} pyrrole and 0.01 g chitosan in a final volume of 10 mL.

A graphite rod from a 2B pencil was isolated with epoxy resin. The exposed area of the graphite electrode was 0.0314 cm^2. Prior to each electropolymerization, the surface of the bare PGE was carefully hand-polished using different grades of emery paper (200–2500 grain). After polishing, the electrode was washed with ethanol and distilled water. Electrochemical deposits were made using a Gamry Potentiostat (Interface 1000) controlled by a personal computer and software (Gamry Framework and Gamry Echem Analyst). A three-electrode setup was used and consisted of a $Ag/AgCl/Cl^-$ reference electrode and platinum wire as a counter-electrode.

The electropolymerization of pyrrole in the presence and absence of chitosan was done potentiodynamically within the potential region of −0.2 V to +0.925 V at a scan rate of 50 mV s^{-1}. To study the influence of the film thickness, the polymeric films synthesized after 3, 5 and 7 cycles on PGE. After polymerization, the coated electrodes were immersed in a 0.5 mol L^{-1} H_2SO_4 solution for 5 min to remove the monomers and other residues.

After the studies of the catalytic activity of the composite films by electrochemical measurements, it was determined that the composite film obtained after 5 cycles was the optimum film thickness (2.1 ± 0.1 μm) for HER. Therefore, the electrodeposition of the Au nanoparticles was performed on the composite film obtained by cyclic voltammetry after 5 cycles in the potential range of −0.5 V to +1.0 V, which was applied for 2 cycles at 50 mV s^{-1} in 0.5 mol L^{-1} H_2SO_4 solution containing 1 mmol L^{-1} $HAuCl_4$. The composite films were ready to use for electrochemical measurements after holding them in the 0.5 mol L^{-1} H_2SO_4 solution for a few minutes.

The electrochemical impedance spectroscopy measurements were performed over a frequency range from 100 kHz to 0.1 Hz at −1.0 V applied potential with a 10 mV Ac amplitude. A FEI Quanta 250 FEG Scanning Electron Microscope (SEM) was used for the morphological analyses.

Results and discussion

In this study, we developed a new, easy to prepare and efficient electrocatalyst for HER. The schematic illustration of the experimental setup is shown in Fig. 1. The catalytic performances of both the PPy-Chi composite films and the PPy-Chi/Au nanostructured composite films coated on PGE were examined by cyclic voltammetry, Tafel polarization curves and electrochemical impedance spectroscopy. All experiments were also carried out on the bare graphite electrode, but due to the uncontrolled hydrogen evolution on it, the obtained data could not be evaluated. Coating the surface of the graphite with a conducting polymer film provided a controllable hydrogen evolution and allowed to decorate this surface with

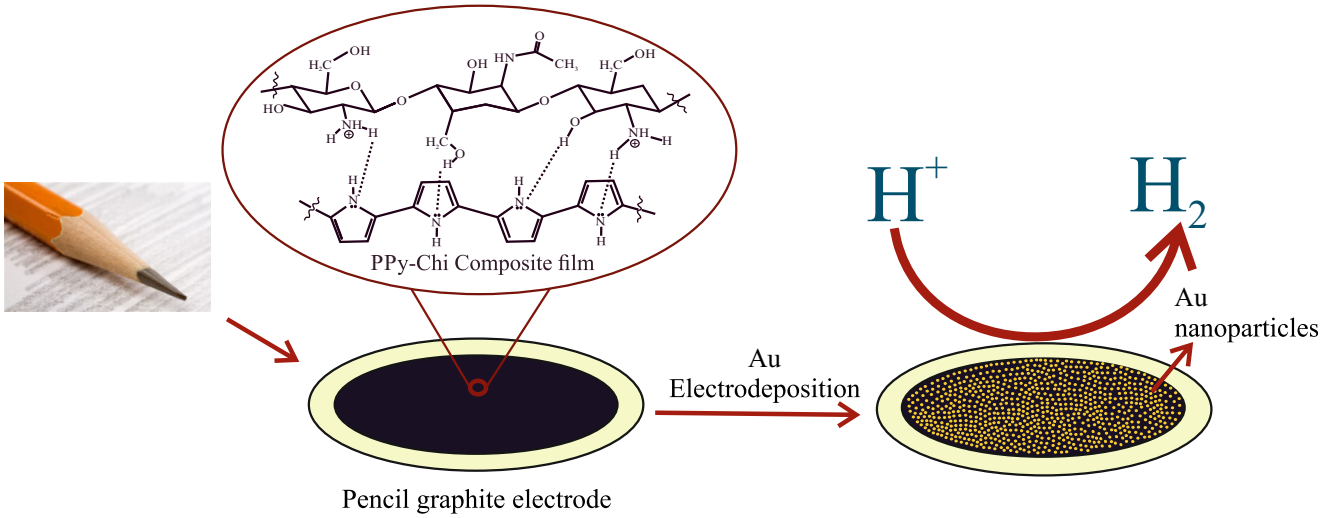

Fig. 1 The schematic illustration of the experimental setup for HER on PGE modified by PPy-Chi/Au

gold nanoparticles homogeneously. The first reason for using gold nanoparticles on PPy-Chi composite surface was to utilize its catalytic activity and the second was to use it at the nano-scale to develop a less expensive electrocatalyst for the hydrogen production. This is the key requirement for an efficient electrocatalyst for hydrogen production.

Morphological analyses

First, the morphological structures of the electrode surfaces were determined by SEM. It is well-known that the size, shape and morphology of the particles affect the catalytic and electrocatalytic properties [3]. Figure 2 presents the details of the morphological structures of the bare pencil graphite as well as the PPy-coated, PPy-Chi-coated and PPy-Chi/Au-coated pencil electrode.

As shown in Fig. 2a, the surface of the graphite has a very porous structure. The typically cauliflower-like morphology of PPy (Fig. 2b) has become more compact with the addition of the chitosan (Fig. 2c). Such a surface is suitable for metal electrodeposition that will end with a homogeneous dispersion of the metal particles. It can be clearly seen that the Au nanoparticles were distributed on the PPy-Chi matrix uniformly (Fig. 2d) and Fig. 2e shows a highly magnified image of the prepared PPy-Chi/Au composite film which indicates the Au deposited on polymeric matrix at the nano-scale. Energy-dispersive spectrometer (EDS) analysis was utilized to determine the composition of the PPy-Chi/Au composite; the results showed that the weight percentage of Au was about 9% (Fig. 2f).

Voltammetric studies

The electrocatalytic performances of the modified electrodes were examined first by cyclic voltammetry, were recorded on the PPy-Chi-coated graphite electrode in the potential range of 0 to −1.5 V in 0.5 mol L^{-1} H_2SO_4 and are shown in Fig. 3a. The modified surface with conducting polymers provides a more controllable hydrogen evolution when compared with the naked electrodes. In addition, the conducting polymers act as a mediator and provide a homogenous distribution of the electrodeposited metals and alloys on their surfaces [20–22].

To determine the optimum film thickness for the hydrogen evolution, all the electrochemical measurements were recorded on different film thicknesses. We know from our previous studies that the polymeric film thickness coated on the electrode surface plays an important role in H^+ adsorption and in reactions such as hydrogenation [32–35]. Therefore, it appears clearly that the obtained current densities are strongly dependent upon the film thickness. The film obtained after 3 cycles of electropolymerization was too thin for H^+ adsorption, while the thicker film obtained after 7 cycles had a low conductivity that decreased the charge transfer ability for H_2 evolution [34, 35]. So, the highest current density response obtained after 5 cycles was the optimum film thickness.

After determining the optimum film, the modification of the PPy-Chi surface with gold nanoparticles was performed as explained in the experimental section. The amount of Au deposited was obtained by the electrical charge consumed during the deposition process Q_{Au} (C cm^{-2}). It was assumed that the current efficiency was 100% for reduction of Au^{3+} and the quantity of deposited Au (m_{Au}) is obtained from the equation; $m_{Au} = Q_{Au}.M_{Au}/nF$, where M is the atomic weight of Au (196.96 g mol^{-1}), n is the number of electrons transferred and F is the Faraday constant (96,485 C mol^{-1}). The loaded Au amount was calculated as 80 μg cm^{-2}.

The real surface area (RSA) of the electrodeposited of Au nanoparticles on the surface of the PPy-Chi composite film can be estimated by simple sweep the modified electrode in

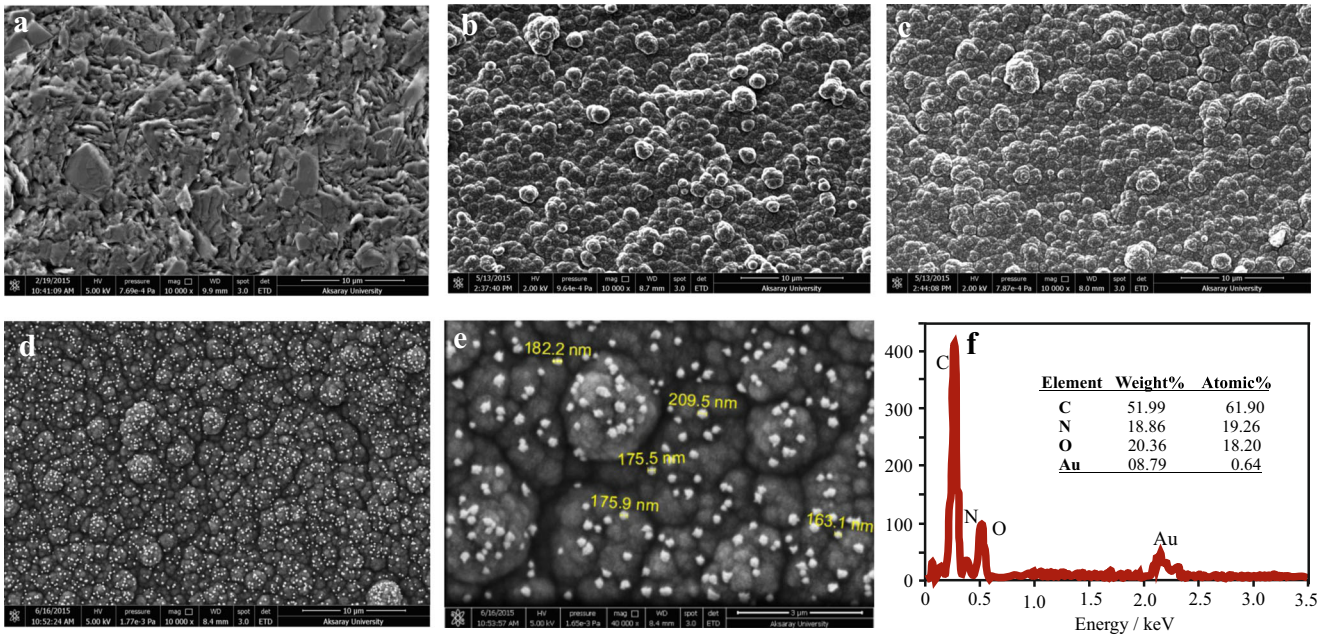

Fig. 2 The SEM images of **a** bare PGE, **b** PGE/PPy, **c** PGE/PPy-Chi, **d** PGE/PPy-Chi/Au, **e** highly magnified image of the PPy-Chi/Au surfaces and **f** EDS spectrum of PPy-Chi/Au composite film

0.5 M H_2SO_4 solution using cyclic voltammetry scanning to −0.5 to 1.5 V at 100 mV s^{-1}. The real surface area of the Au nanoparticles is calculated by assuming that the reduction of a monolayer of gold oxide requires 386 μC cm^{-2} (Q_{ref}) according to RSA = Q/Q_{ref} [36]. The Q for reduction of gold oxide to gold obtained from CV curve is 131.3 μC at observed oxide reduction peak (0.6 V). The real active surface area of the gold nanoparticles on PPy-Chi after 2 cycles is calculated to be 0.34 cm^2.

Then, the comparison of the cyclic voltammograms of the pencil graphite electrodes modified with PPy-Chi and PPy-Chi/Au nano composites was performed in 0.5 mol L^{-1} H_2SO_4 in the same potential window (Fig. 3b). As a reference point, we also performed voltammetric measurements on graphite electrodes that were only coated with PPy. The CVs confirmed that when chitosan was added into the PPy matrix, the obtained current density increased gradually. As stated in the literature, electrical conductivity of the composite material increases with chitosan loading, as well as its thermal stability and the mechanical properties [24, 26–28]. In its actual state, a chitosan film has low electrical conductivity. Although the structure of chitosan monomer has three hydrogens (on -NH_2 and -OH groups), they cannot be mobilized under the action of an electric field to make it a proton conductor. When the hydrogen atoms of chitosan dissolved in acidic medium, they can be mobilized under the influence of an electric field and can bond to PPy; consequently, the obtained film becomes a proton conductor [37, 38]. Also, the interaction between the

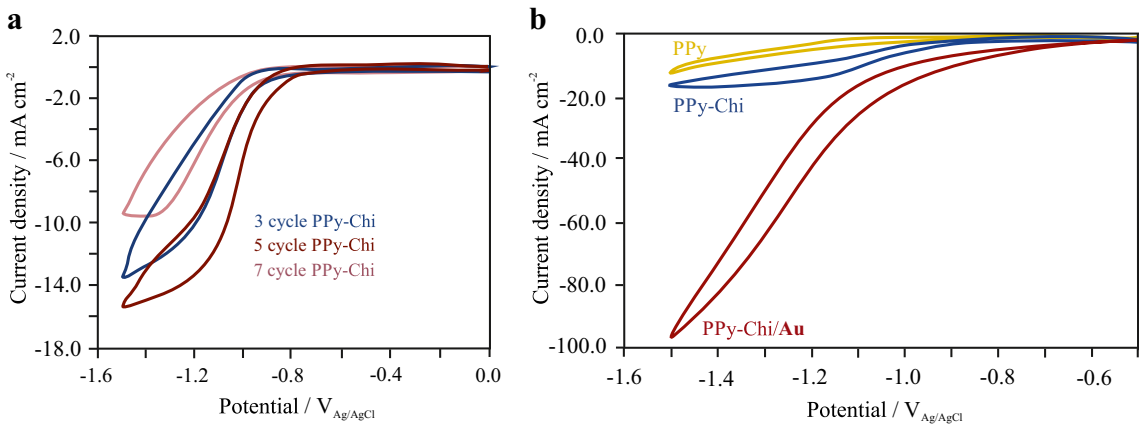

Fig. 3 **a** The cyclic voltammograms of PGE cathode coated with different cycle numbers of PPy-Chi in 0.5 mol L^{-1} H_2SO_4 (ν = 10 mV s^{-1}). **b** The cyclic voltammograms of PGE cathode coated with 5 cycles of PPy, PPy-Chi and PPy-Chi/Au nanoparticles in 0.5 mol L^{-1} H_2SO_4 (ν = 10 mV s^{-1})

PPy and chitosan might result in a more compact structure with small pore size, which provides a better film that results in higher electrical conductivity [39]. The second remarkable point from Fig. 3b is that the obtained current density also increased about five times in the presence of Au nanoparticles, in comparison with the PPy-Chi film from which it is absent. This difference in the current density confirmed that although in small amounts, the Au nanoparticles have a high catalytic effect on HER. The third remarkable point is that the onset potential for hydrogen evolution shifted to the positive potentials when the Au nanoparticles were electrodeposited on the PPy-Chi film. The hydrogen evolution started at about −0.6 V on the PPy-Ci/Au composite film, whereas it occurred near −1.0 V on the PPy-Chi film. The hydrogen evolution took place faster when the potential was more negative than the value of −0.8 V, and there was a sharp rise in the current density observed, which can be attributed to the strong hydrogen evolution in this region. These results accurately demonstrate that the hydrogen evolution requires less energy input and is quite strong on the PPy-Ci/Au composite film when compared with the PPy-Chi film.

Mechanistic investigations

To investigate the performances of the PPy-Chi and PPy-Chi/Au composite films for electroactivity on HER, linear Tafel polarization curves also were obtained (Fig. 4a), and the related kinetic parameters are shown in Table 1 and were calculated from the curves according to the Tafel equation (Eq. 1) [7, 40]. The results obtained on bare Au electrode are also given for the comparison.

$$\eta = a + b\log i = -\frac{2.3RT}{\alpha nF}\log i_0 + \frac{2.3RT}{\alpha nF}\log i \qquad (1)$$

where η represents the applied overpotential, i is the resulting current density, b is the Tafel slope, a is the intercept, i_o is the exchange current density, α is the transfer coefficient, n is the number of transferred electrons, F is the Faraday constant (96,485 C mol^{-1}) and R is the universal gas constant (8.314 J K^{-1} mol^{-1}).

The largest current densities were obtained on the film after 5 cycles of PPy-Chi at each applied potential, which was consistent with the CV results, and the current densities increased noticeably after Au electrodeposition. The hydrogen evolution reaction mechanism is defined by three possible reaction steps in acidic medium. The first step is the Volmer reaction ($H_3O^+ + e^- \rightarrow H_{ad} + H_2O$), and it is the H_{ad} formation step where one electron is transferred with a Tafel slope of ≈120 mV dec^{-1}. This step is followed by either an electrochemical desorption step, which is called the Heyrovsky reaction ($H_{ad} + H_3O^+ + e\text{-} \rightarrow H_2 + H_2O$), with a Tafel slope of ≈40 mV dec^{-1}, or a recombination step, which is called the Tafel reaction ($H_{ad} + H_{ad} \rightarrow H_2$), with a Tafel slope of ≈30 mV dec^{-1} [6, 7].

The Tafel slopes (b) and the current densities (i) calculated by the linear part of the Tafel plots fitted the Tafel equation. The 5 cycles of PPy-Chi composite film showed the smallest Tafel slope, 174 mV dec^{-1} within other composite films, which indicated that the reduction process occurred more easily on this film. The Tafel slope was reduced to 131 mV dec^{-1} by the deposition of the Au nanoparticles on the composite film, and it was calculated about 114 mV dec^{-1} in the case of bare Au electrode. In principle, an electrocatalyst that has a small Tafel slope can generate larger current densities at lower overpotentials. The relatively small slope indicated the fast proton discharge kinetics on the PPy-Chi/Au electrode.

Lu and co-workers studied HER on Au nanoparticle@zinc–iron-embedded porous carbons (Au@Zn–Fe–C). The Tafel Slopes obtained on Au@Zn–Fe–C were in the range of 267 to 130 mV dec^{-1}, depending on the addition of different amount of Au nanoparticles. They have specified that the encapsulated Au nanoparticles play an important role in determining the electrocatalytic activity for HER [41]. Zhang et al.

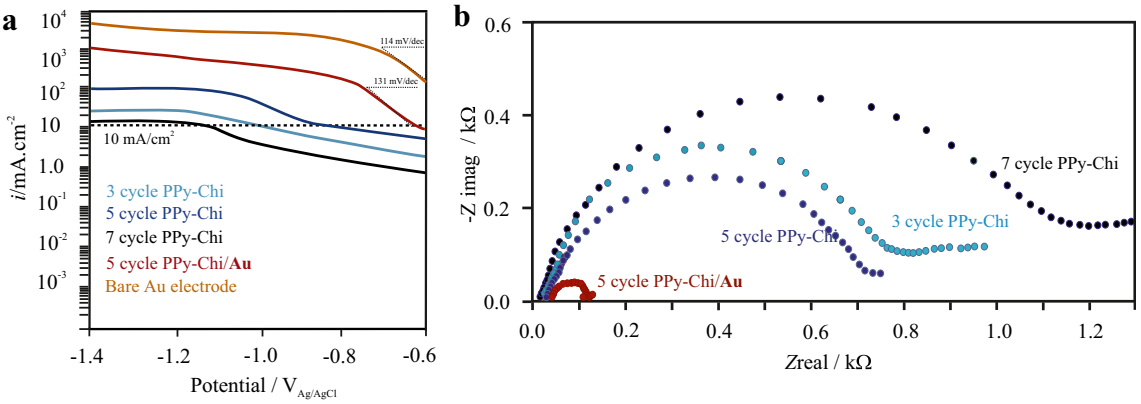

Fig. 4 **a** The Tafel polarization curves of PGE cathode coated with different cycle numbers of PPy-Chi and 5 cycles of PPy-Chi/Au and bare Au electrode in 0.5 mol L^{-1} H_2SO_4 (ν = 10 mV s^{-1}). **b** The Nyquist diagrams of PGE cathode coated with different cycle numbers of PPy-Chi and 5 cycles of PPy-Chi/Au in 0.5 mol L^{-1} H_2SO_4 at −1.0 V

Table 1 The electrochemical parameters calculated from Tafel polarization curves for each composite

Composite	$-b$/mV dec^{-1}	i/mA cm^{-2} ($\eta = -0.9$ V)	$-\eta$/V (10 mA cm^{-2})
3 cycles PPy-Chi	215	7.84	0.99
5 cycles PPy-Chi	174	13.7	0.81
7 cycles PPy-Chi	243	4.43	1.15
5 cycles PPy-Chi/**Au**	131	98.1	0.64
Bare Au electrode	114	1025	0.42

fabricated HER catalysts by integrating gold nanoparticles (AuNPs) on nitrogen-doped carbon nanorods encapsulating carbon nanofibers (AuNPs@NCNRs/CNFs). They also found that the obtained Tafel slopes decreased from 110 to 93 mV dec^{-1} with the increasing amount of $HAuCl_4$ solution [31].

When considering the theoretical values of both the Tafel and Heyrovsky reactions, it is impossible to say that the rate determining step is the Tafel or Heyrovsky reaction according to the calculated values. The Tafel slope of 131 mV dec^{-1} suggested that the hydrogen evolution on the PGE modified by the PPy-Chi/Au composite film probably occurred via a Volmer–Heyrovsky mechanism with the Volmer reaction (hydrogen adsorption) as the rate determining step [4–6].

On the other hand, for the proceeding reaction to occur at a measurable rate, a certain overpotential is required [8]. Therefore, the overpotential at a given current density is a more practical parameter for comparing the hydrogen production rate than the exchange current density itself. The composite film obtained after 5 cycles of PPy-Chi coating at a fixed current density of −10 mA cm^{-2} exhibited a lower overpotential of −0.81 V compared to −0.99 V on the third cycle and −1.15 V on the seventh cycle of the film. This overpotential decreased to −0.64 V on the PPy-Chi/Au film. These prominent differences in the Tafel results prove again the better catalytic behaviour of HER on PPy-Chi/Au compared to PPy-Chi composite film. Another important parameter calculated from the Tafel results was the resulting current density at a fixed applied potential (energy input). The current densities at −0.9 V were determined from the corresponding cathodic current-potential curves for different thicknesses of PPy-Chi composite films. The highest current density is obtained on the fifth cycle of PPy-Chi as 13.7 mA cm^{-2}; this value increased to 98.1 mA cm^{-2} for PPy-Chi/Au composite film (Table 1).

Impedance spectroscopy measurements

For a more detailed examination, electrochemical impedance spectroscopy was employed to compare the charge transfer resistances of the composite films for HER. In the Nyquist plots of the impedance spectra, the semicircles obtained at high frequencies that correspond to the charge transfer resistance are noticeably altered with the film thickness (Fig. 4b). The results are compatible with other electrochemical results and indicate that the smallest resistance was observed on the fifth cycle of the PPy-Chi composite film, so the highest reaction rate of HER occurred on this electrocatalyst. The charge transfer resistance increased at the thinner (the characteristic properties of the naked electrode surface became more dominant) and thicker films (where the conductivity problem of the film arose). After modification of the PPy-Chi composite film (fifth cycle) with Au nanoparticles, the electron transfer resistance reduced more, from 0.7 to 0.1 kΩ (Fig. 4b). The result (0.1 kΩ) for charge transfer is quite good when compared with reference [41]. The decrease in the resistance is evidence for a much faster electron transfer between the composite film and H^+ [42]. This result also confirms again that the rate-control step is the Volmer step: the discharge of a proton to give-up adsorbed hydrogen atoms (H_{ad}).

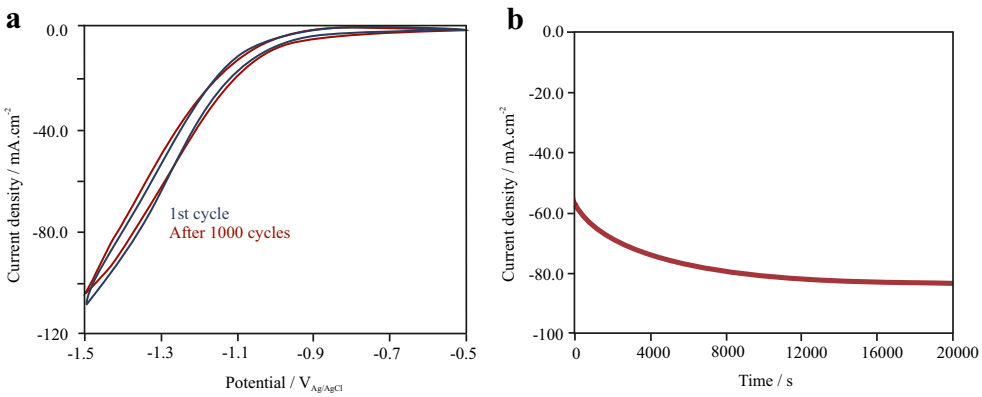

Fig. 5 The stability tests of PPy-Chi/Au in 0.5 mol L^{-1} H_2SO_4. **a** Cyclic voltammograms of the first and after 1000 cycles. **b** Amperometric responses recorded at −1.0 V

Stability studies

Beside the catalytic activity, the stability of an electrocatalyst is also very important. To prove the stability, the H_2 evolution stability test was performed over PPy-Chi/Au composite film, which is a significant parameter for deciding if it is a promising catalyst [43] (Fig. 5).

The continuous cyclic voltammograms were performed from −0.5 to −1.5 V for 1000 cycles at a scan rate of 100 mV s^{-1} in 0.5 mol L^{-1} H_2SO_4 and are shown in Fig. 5a. The polarization curves after 1000 cycles almost overlay the first cycle. In addition, the stability of the current density was tested as a function of time at the −1.0 V applied potential (Fig. 5b). The electrocatalyst maintained its stability over 6 h with a negligible current decrease. After long-term stability and cyclability tests, the results reveal that the PGE modified with PPy-Chi/Au catalyst is stable in acidic solution and suggests the potential use of this catalyst over a long time in electrochemical hydrogen generation.

Conclusion

In conclusion, we fabricated a low-cost, easy modify electrode material and investigated its performance for hydrogen production from water as a model process. A facile pencil graphite electrode was chosen as the support material and modified by electopolymerization of the pyrrole in the presence of a natural biopolymer chitosan at various film thicknesses. The morphological analyses and the catalytic activities of the PPy-Chi coated PGE were examined by cyclic voltammetry, Tafel polarization curves and electrochemical impedance spectroscopy. The optimum film thickness was determined from the experimental results. To utilize the well-known catalytic activity of Au, Au nanoparticles were electrodeposited on the PPy-Chi composite film obtained after 5 cycles of CV. The SEM images showed that the Au nanoparticles were distributed on the composite film homogenously. The electrochemical results obtained from the PPy-Chi/Au demonstrated that the deposited nano-structured Au enhanced the catalytic activity of the composite, which makes it a potentially cost-effective with small amount of nobel metal content, easily prepared and long-term usable material that would use a catalyst for electrocatalytic hydrogen production.

Acknowledgements The authors gratefully acknowledge financial support from The Scientific and Technological Research Council of Turkey (TÜBİTAK) (Project Number TBAG-114Z315), Scientific Research Projects Coordination Unit of Aksaray University (2015-036) and Science and Technological Application and Research Center of Aksaray University.

References

1. Hassan S, Suzuki M, El-Moneim A (2014) A synthesis of MnO_2-chitosan nanocomposite by one-step electrodeposition for electrochemical energy storage application. J Power Sources 246:68–73
2. Hao P, Zhao Z, Leng Y, Tian J, Sang Y, Boughton RI, Wong CP, Liu H, Yang B (2015) Graphene-based nitrogen self-doped hierarchical porous carbon aerogels derived from chitosan for high performance supercapacitors. Nano Energy 15:9–23
3. Chen J, Lim B, Lee EP, Xia Y (2009) Shape-controlled synthesis of platinum nanocrystals for catalytic and electrocatalytic applications. Nano Today 4:81–95
4. Navarro-Flores E, Omanovic S (2005) Hydrogen evolution on nickel incorporated in three-dimensional conducting polymer layers. J Mol Catal A:Chem 242:182–194
5. Dalla Corte DA, Torres C, dos Santos Correa P, Rieder ES, de Malfatti CF (2012) The hydrogen evolution reaction on nickel-polyaniline composite electrodes. Int J Hydrog Energy 37:3025–3032
6. Liao L, Zhu J, Bian X, Zhu L, Scanlon MD, Girault HH, Liu B (2013) MoS_2 formed on mesoporous graphene as a highly active catalyst for hydrogen evolution. Adv Func Mater 23:5326–5333
7. Li Y, Wang H, Xie L, Liang Y, Hong G, Dai H (2011) MoS_2 nanoparticles grown on graphene: an advanced catalyst for the hydrogen evolution reaction. J Am Chem Soc 133:7296–7299
8. Alexis D, Omanovic S (2006) Ni and Ni-Mo hydrogen evolution electrocatalysts electrodeposited in a polyaniline matrix. J Power Sources 158(1):464–476
9. Rheinlander PJ, Herranz J, Durst J, Gasteiger HA (2014) Kinetics of the hydrogen oxidation/evolution reaction on polycrystalline platinum in alkaline electrolyte reaction order with respect to hydrogen pressure. J Electrochem Soc 161(14):F1448–F1457
10. Lu Q, Hutchings GS, Yu W, Zhou Y, Forest RV, Tao R, Rosen J, Yonemoto BT, Cao Z, Zheng H, Xiao JQ, Jiao F, Chen JG (2015) Highly porous non-precious bimetallic electrocatalysts for efficient hydrogen evolution. Nat Commun 6(6567):1–8
11. Zhang Z, Li W, Yuen MF, Ng T-W, Tang Y, Lee C-S, Chen X, Zhang W (2015) Ni-doped MoS_2 nanoparticles as highly active hydrogen evolution electrocatalysts. Nano Energy 18:196–204
12. Shen X, Xia X, Ye W, Du Y, Wang C (2017) Hexagram-like CoS-MoS2 composites with enhanced activity for hydrogen evolution reaction. J Solid State Electrochem 21(2):409–417
13. Tuomi S, Guil-Lopez R, Kallio T (2016) Molybdenum carbide nanoparticles as a catalyst for the hydrogen evolution reaction and the effect of pH. J Catal 334:102–109
14. Chen S, Thind SS, Chen A (2016) Nanostructured materials for water splitting—state of the art and future needs. Electrochem Commun 63:10–17
15. Gong ZQ, Sujari ANA, Ab Ghani S (2012) Electrochemical fabrication, characterization and application of carboxylic multi-walled carbon nanotube modified composite pencil graphite electrodes. Electrochim Acta 65:257–265
16. Sengupta R, Bhattacharya M, Bandyopadhyay S, Bhowmick AK (2011) A review on the mechanical and electrical properties of graphite and modified graphite reinforced polymer composites. Prog Polym Sci 36:638–670
17. Rezaei B, Boroujeni MK, Ensafi AA (2014) A novel electrochemical nanocomposite imprinted sensor for the determination of lorazepam based on modified polypyrrole@sol-gel@gold nanoparticles/pencil graphite electrode. Electrochim Acta 123:332–339
18. Erdem A, Eksin E, Muti M (2014) Chitosan–graphene oxide based aptasensor for the impedimetric detection of lysozyme. Colloids Surf B: Biointerfaces 115:205–211

19. Yuvaraj AL, Santhanaraj D (2014) A systematic study on electrolytic production of hydrogen gas by using graphite as electrode. Mater Res 17:83–87
20. Luo X-L, Xu J-J, Zhang Q, Yang G-J, Chen H-Y (2005) Electrochemically deposited chitosan hydrogel for horseradish peroxidase immobilization through gold nanoparticles self-assembly. Biosens Bioelectron 21(1):190–196
21. Niu L, Li Q, Wei F, Chen X, Wang H (2003) Electrochemical impedance and morphological characterization of platinum-modified polyaniline film electrodes and their electrocatalytic activity for methanol oxidation. J Electroanal Chem 544:121–128
22. Niu L, Li Q, Wei F, Wu S, Liu P, Cao X (2005) Electrocatalytic behavior of Pt-modified polyaniline electrode for methanol oxidation: effect of Pt deposition modes. J Electroanal Chem 578:331–337
23. Lu X, Qiu Z, Wan Y, Hu Z, Zhao Y (2010) Preparation and characterization of conducting polycaprolactone/chitosan/polypyrrole composites. Compos Part A 41:1516–1523
24. Xiang C, Li R, Adhikari B, She Z, Li Y, Kraatz H-B (2015) Sensitive electrochemical detection of salmonella with chitosan-gold nanoparticles composite film. Talanta 140:122–127
25. Yalçınkaya S (2013) Electrochemical synthesis of poly(o-anisidine)/chitosan composite on platinum and mild steel electrodes. Prog Org Coat 76:181–187
26. Marroquin JB, Rhee KY, Park SJ (2013) Chitosan nanocomposite films: enhanced electrical conductivity, thermal stability, and mechanical properties. Carbohydr Polym 92(2):1783–1791
27. Abdi MM, Kassim A, Ekramul Mahmud HNM, Yunus WMM, Talib ZA, Sadrolhosseini AR (2009) Physical, optical, and electrical properties of a new conducting polymer. J Mater Sci 44:3682–3686
28. Li Y, Li G, Peng H, Chen K (2011) Facile synthesis of electroactive polypyrrole–chitosan composite nanospheres with controllable diameters. Polym Inter 60:647–651
29. Li Z, Wua Y, Lua G (2016) Highly efficient hydrogen evolution over $Co(OH)_2$ nanoparticles modified g-C_3N_4 co-sensitized by Eosin Y and Rose Bengal under visible light irradiation. Appl Catal B Environ 188:56–64
30. Wang Y, Sun Y, Liao H, Sun S, Li S, Ager JW III, Xu ZJ (2016) Activation effect of electrochemical cycling on gold nanoparticles towards the hydrogen evolution reaction in sulfuric acid. Electrochim Acta 209:440–447
31. Zhang M, Wang S, Li T, Chen JD, Zhu H, Du ML (2016) Nitrogen and gold nanoparticles co-doped carbon nanofiber hierarchical structures for efficient hydrogen evolution reactions. Electrochim Acta 208:1–9
32. Köleli F, Balun Kayan D (2010) Low overpotential reduction of dinitrogen to ammonia in aqueous media. J Electroanal Chem 638(1):119–122
33. Balun Kayan D, Köleli F (2016) Simultaneous electrocatalytic reduction of dinitrogen and carbon dioxide on conducting polymer electrodes. Appl Catal B Environ 181:88–93
34. Aydın R, Öztürk Doğan H, Köleli F (2013) Electrochemical reduction of carbondioxide on polypyrrole coated copper electro-catalyst under ambient and high pressure in methanol. Appl Catal B Environ 140-141:478–482
35. Çirmi D, Aydın R, Köleli F (2015) The electrochemical reduction of nitrate ion on polypyrrole coated copper electrode. J Electroanal Chem 736:101–106
36. Łukaszewski M, Soszko M, Czerwiński A (2016) Electrochemical methods of real surface area determination of Noble metal electrodes—an overview. Int J Electrochem Sci 11:4442–4469
37. Yahya MZA, Arof AK (2004) Conductivity and X-ray photoelectron studies on lithium acetate doped chitosan films. Carbohydr Polym 55:95–100
38. Mohamed NS, Subban RHY, Arof AK (1995) Polymer batteries fabricated from lithium complexed acetylated chitosan. J Power Sources 56:153–156
39. Gök A, Omastova M, Yavuz AG (2007) Synthesis and characterization of polythiophenes prepared in the presence of surfactants. Synth Met 157:23–29
40. Köleli F, Balun D (2004) Reduction of CO_2 under high pressure and high temperature on Pb-granule electrodes in a fixed-bed reactor in aqueous medium. Appl Catal A:Gen 274:237–242
41. Lu J, Zhou W, Wang L, Jia J, Ke Y, Yang L, Zhou K, Liu X, Tang Z, Li L, Chen S (2016) Core−Shell nanocomposites based on gold nanoparticle@zinc−iron-embedded porous carbons derived from metal−organic frameworks as efficient dual catalysts for oxygen reduction and hydrogen evolution reactions. ACS Catal 6:1045–1053
42. Balun Kayan D, Köleli F (2015) Dinitrogen reduction on a polypyrrole coated. Pt electrode under high-pressure conditions: electrochemical impedance spectroscopy studies Turk J Chem 39(3): 648–659
43. Torabi M, Sadrnezhaad SK (2010) Electrochemical synthesis of flake-like Fe/MWCNTs nanocomposite for hydrogen evolution reaction: effect of the CNTs on dendrite growth of iron and its electrocatalytic activity. Currt Appl Physics 10:72–76